

## COMMUNICATION

## Thermal and electrical conduction in 6.4 nm thin gold films

Cite this: *Nanoscale*, 2013, 5, 4652Huan Lin,<sup>ab</sup> Shen Xu,<sup>a</sup> Chong Li,<sup>a</sup> Hua Dong<sup>c</sup> and Xinwei Wang<sup>\*ac</sup>

Received 8th February 2013

Accepted 29th March 2013

DOI: 10.1039/c3nr00729d

[www.rsc.org/nanoscale](http://www.rsc.org/nanoscale)

For sub-10 nm thin metallic films, very little knowledge is available so far on how electron scattering at surface and grain boundaries reduces the thermal transport. This work reports on the first time characterization of the thermal and electrical conductivities of gold films of 6.4 nm average thickness. The electrical ( $\sigma$ ) and thermal ( $k$ ) conductivities of the Au film are found to be reduced dramatically from their bulk counterparts by 93.7% ( $\sigma$ ) and 80.5% ( $k$ ). Its Lorenz number is measured as  $7.44 \times 10^{-8} \text{ W } \Omega \text{ K}^{-2}$ , almost a twofold increase from the bulk value. The Mayadas–Shatzkes model is used to interpret the experimental results and reveals very strong electron reflection (77%) at grain boundaries.

When the size of metal interconnects is comparable to the electron mean free path, electron transport is dominated by scattering at the metal–dielectric interface, which can significantly reduce the electrical and thermal conductivities.<sup>1–5</sup> Gold thin films are widely used to investigate the mechanisms behind the reduction of electrical and thermal conductivities.<sup>6–8</sup> Compared with the extensive studies of electrical transport, the studies on the in-plane thermal conductivity of nanometer thick gold films are rather scarce. Several experimental studies investigated either the thermal conductivity or the electrical conductivity and used the electrical–thermal analogy to determine the other one.<sup>9</sup> For bulk materials we can use the Wiedemann–Franz (WF) law to calculate the thermal conductivity using an analogy approach between charge transport and heat transport. However, the WF law has not been validated for special metals like nanocrystalline films and their Lorenz numbers can be very different from the corresponding bulk values.<sup>8,10–13</sup> Ou *et al.*<sup>14</sup> calculated the Lorenz number of a

180 nm thick nickel nanowire, and found it to be a little higher than the bulk value. Zhang and co-workers<sup>7,13,15</sup> found that the Lorenz numbers for 15 nm, 28 nm and 48 nm Pt nanofilms are several times larger than the bulk value. Experimental results of Yoneoka *et al.*<sup>16</sup> showed an average Lorenz number of  $3.82 \times 10^{-8}$ ,  $2.79 \times 10^{-8}$  and  $2.99 \times 10^{-8} \text{ W } \Omega \text{ K}^{-2}$  for 7.3, 9.8, and 12.1 nm Pt films, respectively. Zhang and co-workers<sup>7,8</sup> measured the Lorenz numbers of 21–37 nm and 53 nm thick polycrystalline Au films as  $7.0 \times 10^{-8} \text{ W } \Omega \text{ K}^{-2}$  and  $5.0 \times 10^{-8} \text{ W } \Omega \text{ K}^{-2}$  respectively. For very thin films, the measurement of heat conduction and Lorenz numbers becomes very challenging, while such research is very critical to understand the roles of electrons in thermal and electrical conduction with strong interface scattering.

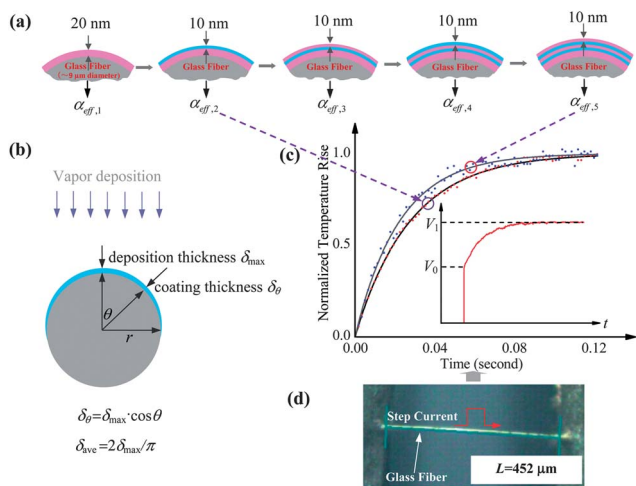
In this work, a technology is developed to achieve a novel capacity of thermal diffusivity/conductivity measurement for thin gold films. In this method, as shown in Fig. 1(a), a micro-glass fiber is used as the base material for supporting the to-be-measured thin gold film. First of all, the glass fiber is coated with one gold film/layer of thickness  $\delta_1 = 20 \text{ nm}$  and the effective thermal diffusivity of the glass fiber–metallic film system (in the axial direction) is measured as  $\alpha_{\text{eff},1}$ . Then the same sample is coated with a second gold layer of thickness  $\delta_2 = 10 \text{ nm}$ , and the sample's thermal diffusivity is measured again as  $\alpha_{\text{eff},2}$ . The increment of the thermal diffusivity induced by the second metallic layer is  $\Delta\alpha_{\text{eff}} = \alpha_{\text{eff},1} - \alpha_{\text{eff},2}$ . This thermal diffusivity difference is directly related to the thermal conductivity of the second gold layer of thickness  $\delta_2$ , and other parameters of the sample. A physical model is developed to determine the thermal conductivity of the metallic layer based on  $\Delta\alpha_{\text{eff}}$ .

Fig. 1(b) shows the profile of the film thickness, and the definition of thicknesses  $\delta_{\text{max}}$  and  $\delta_{\theta}$ . During film preparation, the vapor deposition only coats the top side of the glass fiber and the thickest portion ( $\delta_{\text{max}}$ ) is in the center top. The glass fiber itself is very small in comparison with the whole deposition plume in the sputtering chamber. Therefore it is physically reasonable to assume the gold atom vapor deposits on the glass

<sup>a</sup>Department of Mechanical Engineering, Iowa State University, 2010 Black Engineering Building, Ames, Iowa 50011, USA. E-mail: [xwang3@iastate.edu](mailto:xwang3@iastate.edu); Fax: +1 515 294-3261; Tel: +1 515 294-2085

<sup>b</sup>College of Engineering, Ocean University of China, Qingdao, Shandong, 266100, P. R. China

<sup>c</sup>School of Environmental and Municipal Engineering, Qingdao Technological University, Qingdao, Shandong, 266033, P.R. China



**Fig. 1** (a) Schematic of the cross-section of glass fiber coated with different layers of nm films. Different colors on the glass fiber stand for different layers of the metallic film. (b) The profile of the film thickness and definition of thicknesses  $\delta_{max}$  and  $\delta_\theta$ . (c) Comparison between theoretical fitting (solid curves) and experimental data (dots) for the normalized temperature rise. The inset shows the measured voltage evolution for the sample. (d) The gold coated glass fiber connected between two electrodes.

fiber to be like snow precipitation on a horizontal cylinder. The thickness ( $\delta_\theta$ ) of the metallic layer varies with the location on the fiber surface as  $\delta_\theta = \delta_{max} \cos \theta$ , where  $\theta$  is the angle from the vertical direction. The cross-sectional area of the metallic coating can be expressed as  $A_c = 2 \int_0^{\pi/2} \cos \theta \delta_{max} r d\theta = D \delta_{max}$  and its average thickness,  $\delta_{ave} = 2\delta_{max}/\pi$ .

The transient electro-thermal (TET) technique<sup>17</sup> developed in our laboratory is used in this work to measure the thermal diffusivity of the gold layer-covered micro-glass fiber. The TET technique has been proved to be an effective, accurate, and fast approach to measure the thermal diffusivity of one-dimensional solid materials, both metallic and dielectric. The TET measurement gives results in agreement with reference values with less than 5% difference.<sup>17–21</sup>

A schematic of the TET technology is presented in Fig. 1(d). At the beginning of the experiment, the sample is suspended between two aluminum electrodes. In order to enhance the electrical and thermal contact of the sample to the electrodes, a silver paste is applied at the contact points. The sample is placed in a vacuum chamber to suppress the effect of gas conduction during measurement. During thermal characterization, a step DC current is fed through the wire to generate electric heat. The temperature change of the wire will induce an electrical resistance change, which leads to an overall voltage change of the wire. Therefore the voltage change of the wire can be used to monitor its temperature evolution. As explained in the inset in Fig. 1(c), under the feeding of a square current, the induced voltage profile (red line) undergoes a rapid increase phase and then reaches the steady state, meaning heat transfer equilibrium is established. The transient phase reflects the resistance change of the wire, which in turn gives the idea about

how fast/slow the temperature of the wire evolves. This temperature change is strongly determined by the thermo-physical properties of the wire. Therefore, the transient voltage/temperature change can be used to determine the thermal diffusivity. The sample's voltage evolution ( $V_{sample}$ ) recorded by the oscilloscope is directly related to the average temperature change of the sample. The normalized temperature rise  $T_{exp}^*$  based on the experimental data can be calculated as  $T_{exp}^* = (V_{sample} - V_0)/(V_1 - V_0)$ , where  $V_0$  and  $V_1$  are the initial and final voltages across the sample as shown in Fig. 1(c).  $T^*$  is solved for a one-dimensional heat transfer problem and is expressed as:

$$T^* = \frac{96}{\pi^4} \sum_{m=1}^{\infty} \frac{1 - \exp\left[-(2m-1)^2 \pi^2 \alpha t / L^2\right]}{(2m-1)^4}, \quad (1)$$

where  $\alpha$  and  $L$  are the thermal diffusivity and length of the sample. After  $T_{exp}^*$  is obtained, different trial values of  $\alpha$  are used to calculate the theoretical temperature rise based on eqn (1) and fit the experimental results ( $T_{exp}^*$ ). The value giving the best fit of  $T_{exp}^*$  is taken as the thermal diffusivity of the sample.

To precisely determine the thermal and electrical conductivities of the gold film, physical parameters such as density and specific heat of the glass fiber are required in our data processing. The diameter of glass fibers is measured as  $9.17 \pm 0.54 \mu\text{m}$ . The average density is  $2070 \pm 121 \text{ kg m}^{-3}$ , and the specific heat used in the calculation is  $745 \text{ J kg}^{-1} \text{ K}^{-1}$ .<sup>22</sup> The glass fiber is coated with gold using a sputtering machine (Denton Vacuum Desk V-Standard) which can set the time of sputtering. The film thickness is calibrated by coating gold on a silicon wafer for 20 seconds. The coated silicon wafer is scanned using an atomic force microscope (AFM) and the film thickness is measured at 10 nm.

The electric resistance of  $\delta_{ave} = 6.4 \text{ nm}$  gold films is not stable in the TET experiment. So at the beginning, the glass fiber ( $452 \mu\text{m}$  long) is coated with  $\delta_{max} = 20 \text{ nm}$  gold as the base layer and TET measurement is done on its effective thermal diffusivity. After that, a  $6.4 \text{ nm}$  gold layer ( $\delta_{max} = 10 \text{ nm}$ ) is added every time, and the corresponding effective thermal diffusivity of the fiber is measured. Theoretically, we need to coat only one second layer (10 nm thick) and do measurement for  $\alpha_{eff,2}$ . In order to improve measurement accuracy and significantly suppress experimental uncertainty, we repeat the process of adding a gold layer of 10 nm thickness and measure the corresponding thermal diffusivity  $\alpha_{eff,n}$ . After five TET experiments, five different  $\alpha_{eff}$  and electric resistances are obtained. Fig. 1(c) shows a comparison between the theoretical fitting and experimental data for the normalized temperature rise. It is seen that with 4 layers of 6.4 nm thick gold films on top of the base layer, the normalized temperature rise of the sample goes up faster than that with 1 layer of 6.4 nm gold film, meaning a larger effective thermal diffusivity for the glass fiber with four 6.4 nm thick gold layers. By fitting, the effective thermal diffusivities are determined as  $9.4 \times 10^{-7} \text{ m}^2 \text{ s}^{-1}$  and  $7.3 \times 10^{-7} \text{ m}^2 \text{ s}^{-1}$  for the same glass fiber with 4 and 1 gold layers. The measured effective thermal diffusivity has a relationship with the electrical conductance as follows:

$$\alpha_{\text{eff}} = \alpha + L_{1,\text{Lorenz}}TLR_1^{-1}/(A_w\rho c_p) + L_{2,\text{Lorenz}}TLR_{2,n}^{-1}/(A_w\rho c_p), \quad (2)$$

where  $R_1$  is the resistance of the base layer (20 nm gold coating) and  $R_{2,n}$  ( $n = 1-4$ ) is the resistance of  $n$  layers of  $\delta_{\text{max}} = 10$  nm gold films.  $L_{1,\text{Lorenz}}$  and  $L_{2,\text{Lorenz}}$  are the Lorenz numbers of the base layer and the  $\delta_{\text{max}} = 10$  nm layer. Since  $1/R_{\text{total}} = 1/R_1 + 1/R_{2,n}$  ( $n = 1-4$ ,  $R_{\text{total}}$ : total resistance of the sample), we can get  $R_{2,n}$ . It can be seen from eqn (2) that the effective thermal diffusivity ( $\alpha_{\text{eff}}$ ) changes with the inverse of resistance ( $R_{2,n}^{-1}$ ) linearly and the slope of the fitting line is  $L_{2,\text{Lorenz}}TL/A_w\rho c_p$ . Fig. 2 shows the linear fitting of the four data points. The slope of the fitting line is determined as  $1.01 \times 10^{-4} \text{ m}^2 \text{ s}^{-1} \Omega$ . In the TET experiments the current applied is of 240–400  $\mu\text{A}$  in order to make a temperature rise of the transient stage around 10 K. For  $L_{\text{Lorenz}}$  calculation, an average temperature during the transient state (308 K) is used. With these data, we determine  $L_{\text{Lorenz}}$  of 6.4 nm thick gold film as  $7.44 \times 10^{-8} \text{ W } \Omega \text{ K}^{-2}$  from the equation  $L_{\text{Lorenz}} = A_w\rho c_p\psi/TL$ .

In our experiment, the measured thermal diffusivity has a combined contribution from the glass fiber and the gold layers. The contribution is proportional to their areas. The effective thermal diffusivity of the whole sample is expressed as

$$\alpha_{\text{eff}} = \alpha_w + \frac{1}{(\rho c_p)_w} \frac{4\delta_{1,\text{max}}}{\pi D} [k_1 - \alpha_w(\rho c_p)_c] + \frac{1}{(\rho c_p)_w} \frac{4n\delta_{2,\text{max}}}{\pi D} [k_2 - \alpha_w(\rho c_p)_c], \quad (3)$$

where  $\alpha_w$  is the thermal diffusivity of the glass fiber.  $\delta_{1,\text{max}}$  is 20 nm and is for the base layer,  $k_1$  is the thermal conductivity of the base layer, and  $k_2$  is the thermal conductivity of a single  $\delta_{2,\text{max}} = 10$  nm gold layer. In eqn (3),  $\alpha_{\text{eff}}$  changes with  $n$  linearly and its slope is  $4\delta_{2,\text{max}}[k_2 - \alpha_w(\rho c_p)_c]/\pi D(\rho c_p)_w$ . Fig. 3(a) shows the linear fitting of  $\alpha_{\text{eff}}$  change with the number of Au layers on top of the glass fiber. Linear fitting of these data gives a slope of  $5.5 \times 10^{-8} \text{ m}^2 \text{ s}^{-1}$ . Then the thermal conductivity of Au layers is calculated as  $61.9 \text{ W m}^{-1} \text{ K}^{-1}$ . This value is significantly smaller

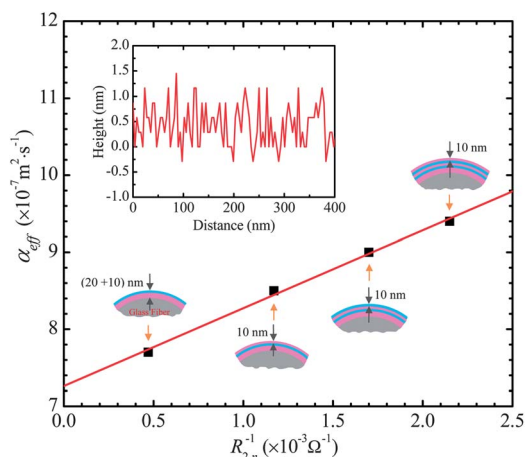


**Fig. 2** Variation of  $\alpha_{\text{eff}}$  of the Au-coated glass fiber (452  $\mu\text{m}$  long) against the inverse of electrical resistance. The red solid line is the linear fitting of the four data points. The inset shows the surface morphology from AFM of 10 nm Au coated on the silicon substrate.

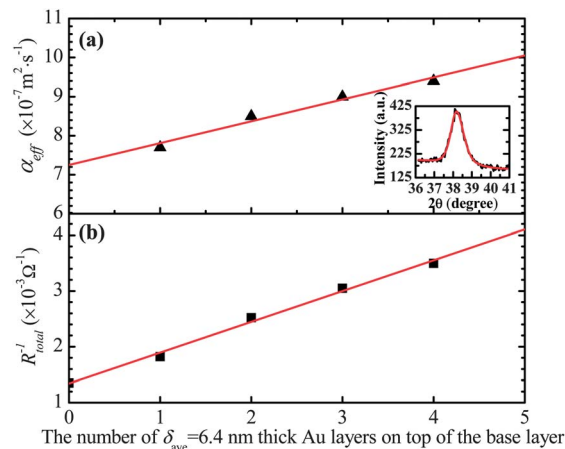


**Fig. 3** Linear fitting (solid lines) of effective thermal diffusivity (a) and inverse of resistance (b) changes against the number of 6.4 nm thick Au layers on top of the base layer. The inset in (a) shows an XRD spectrum of the gold nanofilm.

than the thermal conductivity of bulk Au  $317 \text{ W m}^{-1} \text{ K}^{-1}$  at 308 K.

The total electrical resistance of the Au coating is calculated as

$$\frac{1}{R_{\text{total}}} = \frac{D\delta_{1,\text{max}}\sigma_1}{L} + \frac{Dn\delta_{2,\text{max}}\sigma_2}{L}, \quad (4)$$

where  $\sigma_1$  is the electrical conductivity of the base layer,  $\sigma_2$  is the electrical conductivity of a single  $\delta_{2,\text{max}} = 10$  nm Au layer, and  $n\delta_{2,\text{max}}$  is the total thickness of the layer on top of the base layer. It is evident in eqn (4) that the electrical conductance  $R_{\text{total}}^{-1}$  changes with  $n$  linearly, and its slope is  $D\delta_{2,\text{max}}\sigma_2/L$ . Fig. 3(b) shows the linear fitting of the inverse of resistance against the number of Au layers on top of the base layer. The fitted slope is  $5.52 \times 10^{-4} \Omega^{-1}$ , and the electrical conductivity of the Au layer is calculated as  $2.71 \times 10^6 \Omega^{-1} \text{ m}^{-1}$ . This value is much smaller than the electrical conductivity of bulk Au  $4.34 \times 10^7 \Omega^{-1} \text{ m}^{-1}$  at 308 K, showing the size effect due to very strong electron grain boundary scattering.  $L_{\text{Lorenz}}$  of the gold film can also be calculated as  $7.41 \times 10^{-8} \text{ W } \Omega \text{ K}^{-2}$  based on  $L_{\text{Lorenz}} = k_c/\sigma T$ . This value is very close to  $7.44 \times 10^{-8} \text{ W } \Omega \text{ K}^{-2}$  determined from  $L_{\text{Lorenz}} = A_w\rho c_p\psi/TL$ . From Fig. 3 it is clear that the effective thermal diffusivity and the electrical conductance increase linearly with the number of Au layers, verifying the hypothesis that each deposited film has the same electrical and thermal conductivities and  $\rho c_p$ .

To explore the mechanism behind this significant reduction of thermal and electrical conductivities discussed above, the Mayadas–Shatzkes (MS) model<sup>23,24</sup> is used to understand the strong electron scattering in the nanofilms. Based on the MS model,  $\sigma_f/\sigma_0$  can be approximated by<sup>25</sup>

$$\frac{\sigma_f}{\sigma_0} = \left[ 1 + \frac{3(1-p)}{8k_0} + \frac{7}{5}\alpha \right]^{-1}, \quad (5)$$

within 9% error when the film thickness and the grain diameter are not too small compared with the electron mean free path, i.e.,  $\alpha < 10$  and  $k_0 > 0.1$ .  $\alpha = l_0R/d(1-R)$ ,  $k_0 = \delta_{\text{ave}}/l_0$ ,  $\sigma_f$  and  $\sigma_0$  are

film and bulk electrical conductivities,  $R$  is the electron reflection coefficient at grain boundaries,  $p$  is the specular reflection parameter of electrons at film surfaces,  $l_0$  is the electron mean free path and  $d$  is the average grain size. The MS model is for the film structure in which the grains are in a “columnar” fashion with the column axis normal to the film plane. This is generally true for films deposited by evaporation or sputtering. We characterize the average grain size of the nanofilm by using X-ray diffraction (XRD). The XRD result of the Au nanofilm is shown in the inset of Fig. 3(a), and the average grain size of the Au film is evaluated as 11.2 nm. The grain size is a little larger than the film thickness, supporting the “columnar” grain structure speculation. The inset in Fig. 2 shows surface roughness scanning for gold films on silicon using an atomic force microscope. It can be seen that over a quite long distance  $\sim 50$  nm, the surface has a height change of about 0.75 nm, indicating that the surface is quite flat ( $\sim 3.8^\circ$  variation angle) and smooth in comparison with the electron wavelength ( $\lambda$ ) 0.52 nm in gold [ $\lambda = h/(m_e v_F)$ ,  $v_F = 1.39 \times 10^6$  m s $^{-1}$  (ref. 26)]. Therefore the electron scattering at the film surface is specular, and  $p$  takes the value 1.

Having  $\sigma_0/l_0 = 1.2 \times 10^{15}$   $\Omega^{-1}$  m $^{-2}$  for bulk gold,<sup>27</sup> and the bulk electrical conductivity  $\sigma_0$  as  $4.3 \times 10^7$   $\Omega^{-1}$  m $^{-1}$  at 308 K,<sup>26</sup> the electron mean free path  $l_0$  of Au is calculated as 35.8 nm. This value is close to 41.7 nm (ref. 28) for Au electrons at the Fermi level at room temperature. By fitting our experimental result for electrical conductivity,  $R$  is determined as 0.77. The thermal conductivity with fitted  $R = 0.48$  is 61.7 W m $^{-1}$  K $^{-1}$ . It is obvious that the reflection coefficient  $R$  for the electrical conductivity is much larger than that for the thermal conductivity, indicating that the electron scatterings on the grain boundaries exert different influences on current and heat transport. The  $L_{\text{Lorenz}}$  calculated from the two methods are several times greater than the Sommerfeld value of  $L_0 = 2.45 \times 10^{-8}$  W  $\Omega$  K $^{-2}$ , also indicating that the grain boundary scattering effect imposes greater influence on the charge transport than on the heat conduction. For charge transport, only the electrons quantum mechanically passing through all the boundaries along the background scattering can contribute to the measured electrical conductivity. However, for thermal transport, the scenario becomes different. For those electrons reflected from grain boundaries, they could have energy exchange with the local phonons, thereby leading to thermal transport in space though they have no charge transport contribution. Therefore, the fitted smaller  $R$  for thermal transport reflects this phenomenon. Based on the  $R$  of 0.77 for charge transport, and 0.48 for heat conduction, to first order estimate, it is conclusive that electrons reflected from grain boundaries have about 38% of their energy exchanged with phonons at grain boundaries. The measured thermal conductivity of the Au film is the sum of contributions from electrons ( $k_e$ ) and phonons ( $k_{\text{ph}}$ ). In bulk metal, at room temperature electrons have about 90–95% contribution to the total thermal conductivity, and phonons only have about 5–10%.<sup>29</sup> In the thin Au films studied here, the scenario could change since the electron's contribution is significantly reduced. We have conducted an extensive literature study, but could not find reported results

on the phonon thermal conductivity in nanocrystalline gold films. To give a rough idea about the phonon contribution in thermal transport, we have used non-equilibrium molecular dynamics (MD) simulation to calculate the phonon thermal conductivity ( $k_{\text{ph}}$ ) of gold with 6.4 nm thickness and 11.2 nm size, and observed a  $k_{\text{ph}}$  of 2.08 W m $^{-1}$  K $^{-1}$ . This value is much smaller than the overall thermal conductivity (61.9 W m $^{-1}$  K $^{-1}$ ) of the Au film measured in this work, meaning electron thermal transport is still dominant. This MD result is rather qualitative than quantitative since the temperature gradient is extremely large in modeling ( $>8 \times 10^9$  K m $^{-1}$ ), and the phonon–electron scattering is not considered in classical MD simulation. Also phonon scattering at grain boundaries in real situations could be different from that in a single grain. All these issues should be taken into account in further research to give a quantitative understanding of the phonon transport in ultra-thin nanocrystalline Au films.

During our TET characterization, the experiment is conducted in a vacuum chamber maintained at 30 mTorr. The small effect from the pressure on the measured thermal diffusivity ( $\Delta\alpha_p$ ) had very little influence on the data analysis. This is because in the linear fitting used in the experiment, only the thermal diffusivity increase/change against the film electrical conductance or film thickness is used. In our experiment, the radiation effect exists for all the cases. An increase of the film thickness on the glass fiber will change the radiation from one side since a thicker metallic layer shields more radiation from the fiber surface. Glass and gold have the emissivity of 0.92 and 0.02 respectively at room temperature. The total change of the film thickness from  $\delta_{\text{max}} = 20$  to 60 nm will change the radiation emissivity very little.

In TET characterization, the effect of the small non-uniform and non-constant heating by the resistance change can be expressed as  $-\varepsilon I^2 RL/(A_c \pi^2 \rho c_p)$ , where  $\varepsilon$  is the temperature coefficient of the sample's electrical resistance and  $I$  is the electrical current. In our experiment, the resistance increase by heating is controlled to be around 2% or less. Therefore, the thermal diffusivity change by this non-constant and non-uniform heating is less than  $2 \times 10^{-13}$  m $^2$  s $^{-1}$ , negligible for the experiments. Separate experiments have been conducted to evaluate the electrical contact resistance using the four-probe method. For the glass fibers coated with gold, the silver paste does a good job in securing the contact between the wire and the electrodes with a contact resistance of only a few ohms. Since the glass fiber has a low thermal conductivity, any potential thermal contact resistance between the wire and the base will become negligible compared with the thermal resistance of the sample itself. Also in our experiment, since only the change of the thermal diffusivity and electrical resistance accounts in the linear data fitting, the electrical and thermal contact resistances will remain the same for one sample with different layers of the film, and will have a negligible effect on the final results.

During TET measurement, the characteristic thermal diffusion time is  $\Delta t_1 \sim r^2/\alpha$  ( $r$ : wire radius) in the cross-section direction and  $\Delta t_2 \sim 0.2026 L^2/\alpha$  in the length direction. Take the case of a single layer of 6.4 nm Au on top of the base layer,  $\Delta t_1$  is

estimated to be about 25  $\mu\text{s}$ , and  $\Delta t_2$  is about 0.05 s. It is obvious that  $\Delta t_1 \ll \Delta t_2$ . So during the relative long time temperature evolution of the wire in TET measurement, the heat conduction in the cross-section quickly reaches its equilibrium and the temperature distribution across the glass fiber's cross-section is very uniform. The estimated average temperature rise of the sample during the transient TET stage is around 10 K. In the past, we have done calibration of the temperature coefficient of electrical resistance for sputtering coated gold on a  $\text{TiO}_2$  wire over a very large temperature range ( $>60$  K).<sup>18</sup> The electrical resistance changes with temperature linearly, and the non-linear effect is estimated to be negligible, and will affect our results to a very limited extent. The TET experiment has an uncertainty of fitting and repeatability better than 2.5%.

In summary, the thermal and electrical conductivities ( $k$  and  $\sigma$ ) of Au films with an average thickness of 6.4 nm were characterized successfully. The results showed that  $k$  ( $=61.9 \text{ W m}^{-1} \text{ K}^{-1}$ ) and  $\sigma$  ( $=2.71 \times 10^6 \text{ } \Omega^{-1} \text{ m}^{-1}$ ) are reduced by 80.5% and 93.7% compared to bulk Au. In such ultra-thin Au films, the thermal transport is still dominated by electrons. The much stronger reduction in  $\sigma$  significantly increased  $L_{\text{Lorenz}}$  to  $7.44 \times 10^{-8} \text{ W } \Omega \text{ K}^{-2}$ , about a twofold increase from the bulk value.

## Acknowledgements

Support of this work from the Office of Naval Research (N000141210603), the Army Research Office (W911NF-12-1-0272), and the National Science Foundation (CBET-0931290) is gratefully acknowledged. We are grateful to MO-SCI Corporation for providing the glass fiber samples used in this work. H.L. is supported by the China Scholarship Council.

## References

- 1 K. Fuchs, *Proc. Cambridge Philos. Soc.*, 1938, **34**, 100–108.
- 2 E. H. Sondheimer, *Adv. Phys.*, 1952, **1**, 1–42.
- 3 S. B. Soffer, *J. Appl. Phys.*, 1967, **38**, 1710–1715.
- 4 Y. Namba, *Jpn. J. Appl. Phys., Part 1*, 1970, **9**, 1326–1329.
- 5 S. R. Gurrum, Y. K. Joshi, W. P. King and K. Ramakrishna, *IEEE Electron Device Lett.*, 2004, **25**, 696–698.
- 6 S. P. Gurrum, W. P. King, Y. K. Joshi and K. Ramakrishna, *J. Heat Transfer*, 2008, **130**, 082403.
- 7 H. D. Wang, J. H. Liu, X. Zhang, Z. Y. Guo and K. Takahashi, *Heat Mass Transfer*, 2011, **47**, 893–898.
- 8 Q. G. Zhang, B. Y. Cao, X. Zhang, M. Fujii and K. Takahashi, *Phys. Rev. B: Condens. Matter Mater. Phys.*, 2006, **74**, 134109.
- 9 P. Nath and K. L. Chopra, *Thin Solid Films*, 1974, **20**, 53–62.
- 10 I. S. Beloborodov, A. V. Lopatin, F. W. J. Hekking, R. Fazio and V. M. Vinokur, *Europhys. Lett.*, 2005, **69**, 435–441.
- 11 N. Stojanovic, D. H. S. Maithripala, J. M. Berg and M. Holtz, *Phys. Rev. B: Condens. Matter Mater. Phys.*, 2010, **82**, 075418.
- 12 V. Tripathi and Y. L. Loh, *Phys. Rev. Lett.*, 2006, **96**, 046805.
- 13 X. Zhang, H. Q. Xie, M. Fujii, H. Ago, K. Takahashi, T. Ikuta, H. Abe and T. Shimizu, *Appl. Phys. Lett.*, 2005, **86**, 171912.
- 14 M. N. Ou, T. J. Yang, S. R. Harutyunyan, Y. Y. Chen, C. D. Chen and S. J. Lai, *Appl. Phys. Lett.*, 2008, **92**, 063101.
- 15 X. Zhang, Q. G. Zhang, B. Y. Cao, M. Fujii, K. Takahashi and T. Ikuta, *Chin. Phys. Lett.*, 2006, **23**, 936–938.
- 16 S. Yoneoka, J. Lee, M. Liger, G. Yama, T. Kodama, M. Gunji, J. Provine, R. T. Howe, K. E. Goodson and T. W. Kennyt, *Nano Lett.*, 2012, **12**, 683–686.
- 17 J. Q. Guo, X. W. Wang and T. Wang, *J. Appl. Phys.*, 2007, **101**, 063537.
- 18 X. Feng, X. Wang, X. Chen and Y. Yue, *Acta Mater.*, 2011, **59**, 1934–1944.
- 19 X. H. Feng, X. P. Huang and X. W. Wang, *Nanotechnology*, 2012, **23**, 185701.
- 20 X. H. Feng and X. W. Wang, *Thin Solid Films*, 2011, **519**, 5700–5705.
- 21 J. Q. Guo, X. W. Wang, L. J. Zhang and T. Wang, *Appl. Phys. A: Mater. Sci. Process.*, 2007, **89**, 153–156.
- 22 F. P. Incropera, *Fundamentals of heat and mass transfer*, John Wiley, Hoboken, NJ, 6th edn, 2007.
- 23 A. F. Mayadas and M. Shatzkes, *Phys. Rev. B: Solid State*, 1970, **1**, 1382–1389.
- 24 A. F. Mayadas, M. Shatzkes and J. F. Janak, *Appl. Phys. Lett.*, 1969, **14**, 345–347.
- 25 T. Q. Qiu and C. L. Tien, *J. Heat Transfer*, 1993, **115**, 842–847.
- 26 C. Kittel, *Introduction to solid state physics*, Wiley, New York, 5th edn, 1976.
- 27 J. Vancea, H. Hoffmann and K. Kastner, *Thin Solid Films*, 1984, **121**, 201–216.
- 28 S. Kumar and G. C. Vradis, *J. Heat Transfer*, 1994, **116**, 28–34.
- 29 R. Fletcher and D. Greig, *Philos. Mag.*, 1967, **16**, 303–315.